

Geophysical Research Letters



RESEARCH LETTER

10.1029/2021GL094333

Key Points:

- On average, urban NO₂ inequalities of ~28% are observed with race-ethnicity and income; disparities are much greater in many cities
- Diesel traffic is the dominant source of NO₂ disparities; a 62% reduction in diesel emissions would decrease inequalities by more than 37%
- TROPOMI observations combined with oversampling resolve surface patterns in NO₂ disparities at the census-tract scale

Supporting Information:

Supporting Information may be found in the online version of this article.

Correspondence to:

S. E. Pusede,
sepusede@virginia.edu

Citation:

Demetillo, M. A. G., Harkins, C., McDonald, B. C., Chodrow, P. S., Sun, K., & Pusede, S. E. (2021). Space-based observational constraints on NO₂ air pollution inequality from diesel traffic in major US cities. *Geophysical Research Letters*, 48, e2021GL094333. <https://doi.org/10.1029/2021GL094333>

Received 18 MAY 2021

Accepted 10 AUG 2021

© 2021. The Authors.

This is an open access article under the terms of the [Creative Commons Attribution-NonCommercial-NoDerivs License](#), which permits use and distribution in any medium, provided the original work is properly cited, the use is non-commercial and no modifications or adaptations are made.

Space-Based Observational Constraints on NO₂ Air Pollution Inequality From Diesel Traffic in Major US Cities

Mary Angelique G. Demetillo¹ , Colin Harkins^{2,3} , Brian C. McDonald³, Philip S. Chodrow⁴ , Kang Sun^{5,6} , and Sally E. Pusede¹

¹Department of Environmental Sciences, University of Virginia, Charlottesville, VA, USA, ²Cooperative Institute for Research in Environmental Sciences, University of Colorado, Boulder, CO, USA, ³NOAA Chemical Sciences Laboratory, Boulder, CO, USA, ⁴Department of Mathematics, University of California Los Angeles, Los Angeles, CA, USA, ⁵Department of Civil, Structural and Environmental Engineering, University at Buffalo, Buffalo, NY, USA, ⁶Research and Education in eEnergy, Environment and Water (RENEW) Institute, University at Buffalo, Buffalo, NY, USA

Abstract Air pollution disproportionately burdens communities of color and lower-income communities in US cities. We have generally lacked city-wide concentration measurements that resolve the steep spatiotemporal gradients of primary pollutants required to describe intra-urban air pollution inequality. Here, we use observations from the recently launched TROPospheric Ozone Monitoring Instrument (TROPOMI) satellite sensor and physics-based oversampling to describe nitrogen dioxide (NO₂) disparities with race, ethnicity, and income in 52 US cities (June 2018–February 2020). We report average US-urban census tract-level NO₂ inequalities of $28 \pm 2\%$ (race-ethnicity and income combined), with many populous cities experiencing even greater inequalities. Using observations and inventories, we find diesel traffic is the dominant source of NO₂ disparities, and that a 62% reduction in diesel emissions would decrease race-ethnicity and income inequalities by 37%. We add evidence that TROPOMI resolves tract-scale NO₂ differences using relationships with urban segregation patterns and spatial variability in column-to-surface correlations.

Plain Language Summary People of color and people with lower household incomes commonly experience higher levels of air pollution and worsened health burdens from poor air quality in US cities. We have lacked direct observations of air pollution across cities with which to describe, explain, and guide policymaking on air pollution disparities. Nitrogen dioxide is an important combustion pollutant that is co-emitted with many other toxic pollutants, and its concentrations are highly variable between neighborhoods. Here, we use nitrogen dioxide measurements collected from space by the TROPospheric Ozone Monitoring Instrument (TROPOMI) to describe inequalities within 52 US cities. TROPOMI captures greater spatial detail than previously possible, and the near-daily data collection allows for interpretation of the specific polluting sources causing nitrogen dioxide inequality, including diesel traffic emissions. Because satellite applications for air pollution inequality analyses are nascent, we build on our past work to advance understanding of the extent to which TROPOMI resolves inter-neighborhood nitrogen dioxide differences.

1. Introduction

In US cities, the concentrations of many air pollutants have been observed, modeled, and inferred to be higher in neighborhoods where residents are primarily people of color and have lower household incomes (e.g., Ard, 2015; Bell & Ebisu, 2012; Bullard, 1987; Gwynn & Thurston, 2001; Jerrett et al., 2005; O'Neill et al., 2003; Pope et al., 2016; Tessum et al., 2019). These disparities have been shown to cause measurable differences in health and life expectancy (Adar & Kaufman, 2007; Di et al., 2017; Lin et al., 2002; Lipfert & Wyzga, 2008). Heavy-duty diesel vehicles (HDDVs) are a major driver of air pollution inequalities (Demetillo et al., 2020; Houston et al., 2004, 2008, 2011, 2014; Lena et al., 2002; J. I. Levy et al., 2009; Nguyen & Marshall, 2018; Tessum et al., 2021), with HDDV exhaust containing nitrogen oxides (NO_x ≡ NO + NO₂) and a myriad of hazardous co-emissions (HEI, 2010). Source characterization of air quality disparities,

including from diesel traffic emissions, has been hindered by the lack of city-wide measurements resolving steep atmospheric pollutant gradients and providing temporal information useful for source identification.

Nitrogen dioxide (NO_2) is a combustion product and a key control over atmospheric oxidation and secondary pollutant formation. Communities of color and those with lower household incomes often experience elevated NO_2 concentrations and exposures (Clark et al., 2014, 2017; Kerr et al., 2021; Kravitz-Wirtz et al., 2016; Rosofsky et al., 2018; Southerland et al., 2021). Epidemiological studies indicate an association between NO_2 exposure and/or its co-emissions and various adverse health effects (Brook et al., 2007; Brunekreef & Holgate, 2002; Burnett et al., 2004). NO_2 is a common surrogate for combustion pollution generally (I. Levy et al., 2014) and toxins in traffic exhaust specifically (HEI, 2010). HDDVs contribute a major portion of urban NO_x despite being a small fraction (3%–6%) of the US fleet in terms of distance traveled, as diesel engines produce $\times 7$ more NO_x per kg fuel burned than gasoline (McDonald et al., 2012, 2018). Because its sources are ubiquitous and distributed, NO_2 is highly variable in space and time, with typical distance-decay gradients away from sources of <0.5 – 2 km (Apte et al., 2017; Choi et al., 2012; Karner et al., 2010). A key advantage to focusing air pollution inequality analyses on NO_2 is that it has recently become possible to observe NO_2 daily from space at the scale of a few kilometers using the TROPospheric Ozone Monitoring Instrument (TROPOMI).

In Demetillo et al. (2020), we conducted a detailed evaluation of the use of TROPOMI observations to describe intra-urban NO_2 disparities, demonstrating that TROPOMI was indeed well-positioned to inform multiple aspects of NO_2 inequality research in Houston, Texas. We used fine spatial resolution ($250 \times 500 \text{ m}^2$) airborne NO_2 remote sensing measurements from the GEOstationary Coastal and Air Pollution Events Airborne Simulator (GCAS) as a standard (Nowlan et al., 2018), showing that TROPOMI, oversampled to $0.01^\circ \times 0.01^\circ$ using the physics-based algorithm employed here, resolved equivalent NO_2 relative inequalities as GCAS. We assessed the effects of observational uncertainties, retrieval biases, and time averaging on NO_2 inequality estimates, finding that although their influence led to underestimations in absolute census tract-level differences, TROPOMI still captured key variations in NO_2 spatial distribution between tracts. We also showed that spatial patterns in NO_2 columns reflected those at the surface, an essential aspect of their application to air quality environmental justice decision-making, and determined that column-based inequalities represented those that would be captured at the surface.

Here, we expand this application of TROPOMI, describing NO_2 inequality in 52 major US cities and using these observations as empirical constraints on the contribution of HDDV traffic to NO_2 disparities. We report neighborhood-level (census-tract) disparities with race, ethnicity, and income over an almost 2-year period (June 2018–February 2020). We analyze weekday-weekend differences from both TROPOMI and NO_x emissions inventories to quantify the role of diesel traffic in NO_2 inequalities. We discuss results seasonally, as the NO_2 atmospheric lifetime is shorter in the summer, leading to greater co-location between NO_x emission sources and NO_2 columns than in the winter. We further explore analytical issues in the use of TROPOMI for observing tract-scale inequalities in cities where higher spatial resolution measurements are not available, investigating inequality relationships with urban segregation patterns, and correlating column and surface measurements as a function of their spatial coincidence.

2. Data and Methods

2.1. TROPospheric Ozone Monitoring Instrument (TROPOMI)

TROPOMI detects various atmospheric trace gases in the ultraviolet and visible, near-infrared, and short-wave infrared spectral regions (van Geffen et al., 2018; Veeffkind et al., 2012). TROPOMI samples at $\sim 1:30$ p.m. local time (LT) almost daily from onboard the sun-synchronous Copernicus Sentinel-5 Precursor satellite. NO_2 is retrieved by fitting the 405–465 nm band using an updated OMI DOMINO algorithm based on the QA4ECV project (Boersma et al., 2011, 2018; Lorente et al., 2017; van Geffen et al., 2015; Zara et al., 2018). Before August 6, 2019, NO_2 was retrieved at a nadir spatial resolution of $3.5 \times 7 \text{ km}^2$. NO_2 tropospheric vertical column densities (TVCDs) have since become available at $3.5 \times 5.5 \text{ km}^2$. Precision of individual TVCDs over polluted scenes is on the order of 30%–60% (Boersma et al., 2018) and dominated by uncertainties in air mass factor inputs, including clouds, NO_2 profile shape (daily $1^\circ \times 1^\circ$ TM5-MP output) (Williams et al., 2017), and surface albedo (monthly $0.5^\circ \times 0.5^\circ$ OMI climatology) (Kleipool et al., 2008).

We use the TROPOMI Level 2 NO₂ product averaged to 0.01° × 0.01° (~1 × 1 km²) with a physics-based oversampling algorithm (Sun et al., 2018). We include cloud-free scenes with qa > 0.75. We calculate mean NO₂ TVCDs within census tract boundaries for 52 US cities (Table S1) over June 2018–February 2020, summer (June–August), and winter (December–February), and separately analyze seasonal NO₂ TVCDs on weekdays and weekends. We define weekdays as Tuesdays–Fridays and weekends as Saturdays–Sundays. Monday and Saturday are considered transition days as they are influenced by carryover of yesterday's NO₂. We remove Mondays from our analysis for this reason but keep Saturdays to improve weekend statistics. The mean number of TROPOMI pixels rounded up to the nearest integer in each 0.01° × 0.01° grid are as follows (±1 σ standard deviation), 77 ± 24 (summer weekdays), 33 ± 10 (summer weekends), 33 ± 21 (winter weekdays), and 18 ± 11 (winter weekends), with reduced wintertime sampling statistics due to increased cloud cover (Table S2). TROPOMI observations are spatially continuous (discretized to 0.001° × 0.001°), giving NO₂ TVCDs within tracts smaller than 1 km². Cities were selected to represent both the largest US urban areas and mid-sized cities giving broad country-wide coverage. Cities are defined as US Census-designated “urbanized areas” (UAs) with two exceptions: we separate New York–Newark, NJ–NY–CT along state lines into New York City, NY and Newark, NJ and San Francisco–Oakland, CA along the San Francisco Bay into San Francisco and Oakland, CA. With a population density threshold of 1,000 people mi⁻², UAs represent the urban core of metropolitan areas; therefore, results reflect intra-urban rather than urban-suburban differences (Demetillo et al., 2020).

2.2. Population-Weighted Census-Tract NO₂ Inequalities

We calculate population-weighted NO₂ census tract-averaged TVCDs with race and ethnicity and sort tracts by household poverty status or median household income using the US Census database for 2019 (Text S1). Race-ethnicity groups are defined following the US Census categories of Black and African Americans, Asians, American Indians and Native Alaskans, referred to in the text as Native Americans, and whites, excluding people from each racial group identifying as Hispanic or Latino, and Hispanics/Latinos, including all races also reporting as Hispanic and/or Latino. Poverty status is defined according to the US Census Bureau definition using the household income-to-poverty ratio. Households are categorized as below the poverty line if their income is below the US Federal Poverty Guidelines threshold, which scales with the number of people per household. Tracts are classified as follows: below the poverty line, >20% of tract households at or below an income-to-poverty ratio of one; near poverty, all tract households having an income-to-poverty ratio of 1–1.24; and above poverty, all tract households having an income-to-poverty ratio >1.24. We discuss the sensitivity of our results to the 1.24 threshold in Text S1. We combine race-ethnicity and income categories, reporting results for Black and African Americans, Asians, Native Americans, and/or Hispanic/Latino residents in the lowest median income quintile tracts (LINs) and for non-Hispanic/Latino whites residing in the highest median income quintile tracts (HIWs). Household income quintiles are UA specific.

2.3. NO_x Inventories

The Fuel-based Inventory from Vehicle Emissions (FIVE18–19) is a US-wide, 4 × 4 km² mobile source (on-road and off-road, gasoline and diesel engines) NO_x emissions inventory providing monthly mean hourly data on weekdays, Saturdays, and Sundays (Harkins et al., 2021; McDonald et al., 2012, 2018). Emission rates are based on publicly available fuel sales reports, road-level traffic counts, and time-resolved weigh-in-motion traffic counts. Fuel-use uncertainties are determined from differences between fuel sale reports and truck travel and traffic count site-selection and sample size. Emissions uncertainties are ±16% and ±17% for gasoline and diesel vehicles, respectively, and are derived from a regression analysis of near-road infrared remote sensing and tunnel studies (Jiang et al., 2018). Fuel sales reports are provided at the state level, and we utilize separate link-level traffic counting data sets of light-duty and heavy-duty traffic (FHWA, 2020), downscaling to 4 × 4 km² following McDonald et al. (2014). Traffic counting data sets are estimated to spatially resolve ~70% of passenger vehicles and ~80% of heavy-duty truck traffic. The small remainder (20%–30%) is spatially allocated using population as a surrogate. The additional uncertainty associated with downscaling traffic results in higher urban-scale emission uncertainties of ±24% for gasoline and ±24% for diesel vehicles (McDonald et al., 2014).

NO_x stationary source emissions are from the 2017 National Emissions Inventory (NEI17) updated January 2021 Version (EPA, 2021). The NEI17 reports annual emission totals of point sources including industrial facilities, electricity generating units, oil and gas operations, and airports. Data for smaller industrial facilities, for example, dry cleaners and gas stations, are voluntarily submitted by state agencies and counted as area rather than point sources. Here, we focus on annual NEI17 point source emissions and assume they exhibit no seasonal or day-to-day variability. A comparison of monthly time-resolved NEI point source NO_x emissions in July and January indicated differences are indeed small ($\sim 5\%$). Emissions uncertainties in power plants are $\pm 25\%$ (Frost et al., 2006); uncertainties in industrial facilities and other stationary sources are larger and assumed to be $\pm 50\%$ (Jiang et al., 2018).

2.4. Segregation Extent and Structure

We compute three complementary metrics to quantify and describe city-level racial segregation extent and structure, with segregation structure classified as clustered (mega-regions of segregation) or patch worked (micro-regions of segregation), based on the same 2019 US Census tract-level demographics and UA boundaries as the inequality results. We calculate the Shannon Entropy Index, a measure of diversity and prevalence. Cities with low entropy have a small number of prominent groups, whereas cities with high entropy have roughly equal proportions of groups (Reardon & Firebaugh, 2002). We describe the extent of urban segregation through the Information Theory Index (Reardon & Firebaugh, 2002; Theil & Finizza, 1971), reflecting the amount of information that an individual's location carries about their demographic group. This is an aspatial metric describing the extent of segregation by comparing the demographic representation of a geographic unit to the overall city average (Reardon & O'Sullivan, 2004; Roberto, 2015). We compute the mean local information density, a measure of the spatial scale of segregation, generating urban segregation structure estimates based on the Fisher information between spatial and demographic variables (Chodrow, 2017).

2.5. Surface NO_2^* Measurements

We use NO_2^* surface measurements from 97 non-roadway monitors in 20 UAs identified as having at least three NO_2 monitoring stations operating during June 2018–February 2020 (Table S3). Almost all of these NO_2 instruments operate by first decomposing NO_2 to NO over a heated molybdenum catalyst and measuring NO by chemiluminescence. NO_2 data collected with this technique have a known positive interference from oxidized and reduced nitrogen compounds, which also thermally decompose across the catalyst but at non-unity efficiency (Dunlea et al., 2007). The nomenclature NO_2^* is used in acknowledgment of this interference. Past research has shown the instruments capture NO_2 temporal patterns (Russell et al., 2010) and NO_2 mixing ratios before substantial oxidation has occurred. Because we are interested in the distance dependence of correlations between surface NO_2^* and the overhead TROPOMI TVCDs, rather than the surface NO_2 mixing ratios themselves, we do not apply a correction factor to the NO_2^* data set.

3. Results and Discussion

3.1. NO_2 Inequality and the Role of Diesel NO_x Emissions

Across the 52 cities in our study, representing 130 million residents, population-weighted NO_2 TVCDs are on average $17 \pm 2\%$ higher for Black and African Americans, $19 \pm 2\%$ higher for Hispanics/Latinos, $12 \pm 2\%$ higher for Asians, and $15 \pm 2\%$ higher for Native Americans compared to whites (city-level results are weighted by urban population size in the averaging). NO_2 TVCDs are on average higher for people living below ($17 \pm 2\%$) and near the poverty line ($10 \pm 2\%$) than for those above. When race-ethnicity and income are combined, we report an average of $28 \pm 2\%$ greater population-weighted NO_2 for LINs than HIWs, with the highest inequalities observed in Phoenix, Arizona ($46 \pm 2\%$), Los Angeles, California ($43 \pm 1\%$), and Newark, New Jersey ($42 \pm 2\%$) (Figure 1). In only one city, San Antonio, Texas, is the sign of LIN-HIW inequality negative over June 2018–February 2020 ($-6 \pm 3\%$), although a small number of negative values are also observed for the other metrics. In the five most-populated UAs, representing $\sim 35\%$ of the population, NO_2 TVCDs are $36 \pm 3\%$ higher for LINs compared to HIWs. Absolute NO_2 disparities (molecules cm^{-2}) are strongly associated with local city-level NO_2 pollution (Figure 1h), with a Pearson correlation coefficient

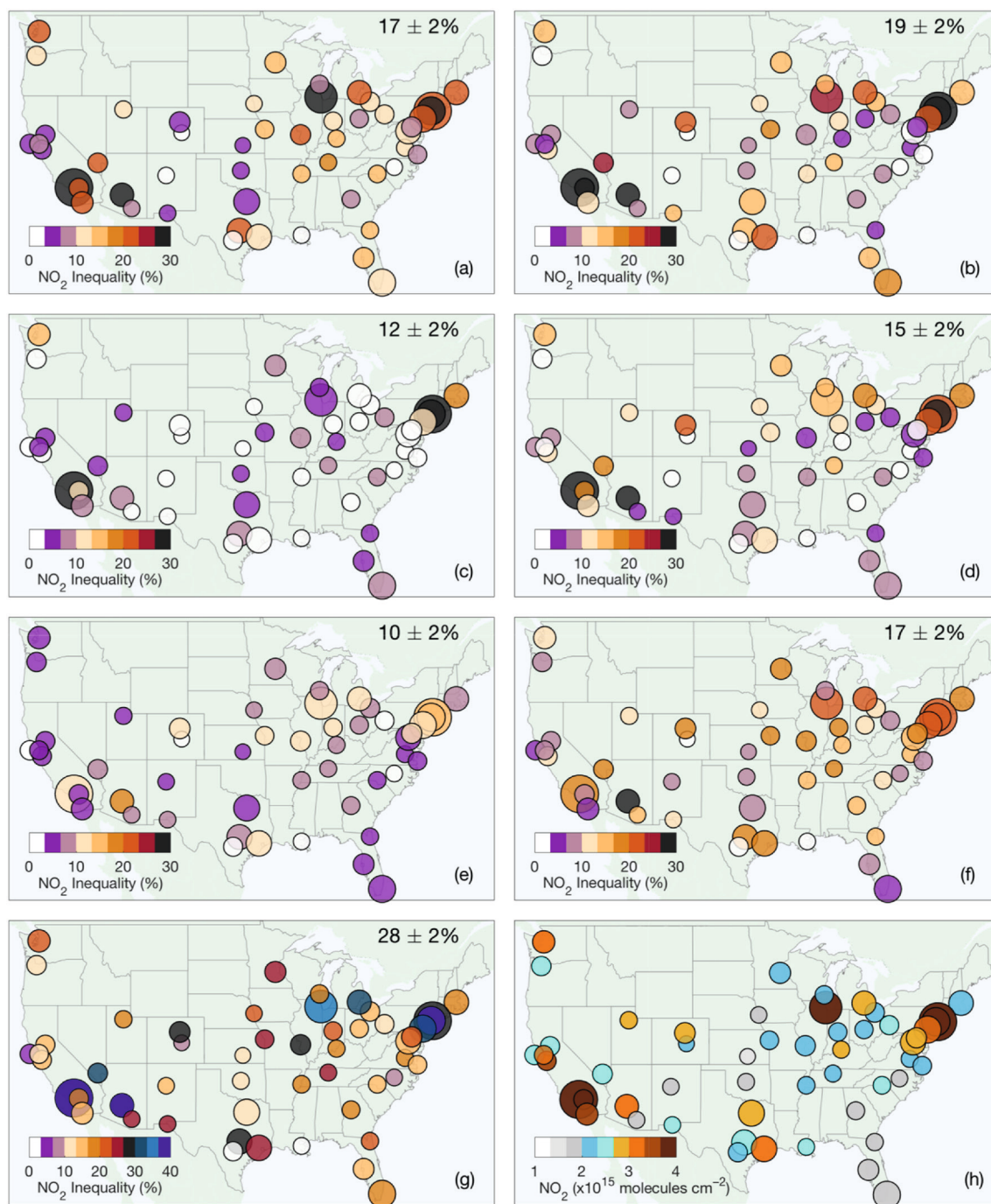


Figure 1. Relative NO₂ inequalities (percentage difference between population-weighted NO₂ means) for 52 major US cities over all days in June 2018–February 2020. Marker size reflects the total city population with the smallest markers representing cities with <1.5 million residents and the largest markers for cities with >10 million residents. Average NO₂ inequalities are shown for Black and African American (a), Hispanic/Latino (b), Asian (c), and Native American (d) compared to white residents. Inequalities are also mapped for people living near (e) and below (f) versus above the poverty line and for LINs compared to HIWs (g). Displayed mean values for each group are weighted by urban population size. City-averaged NO₂ tropospheric vertical column densities are shown (h).

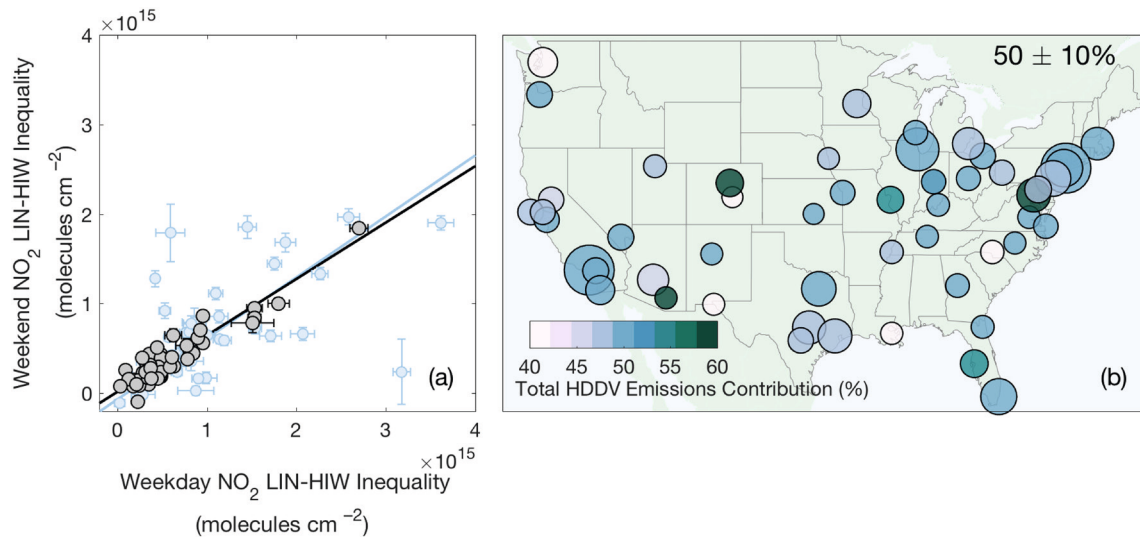


Figure 2. Absolute differences (molecules cm⁻²) in population-weighted NO₂ TVCDs between LINs and HIWs on weekdays and weekends (a) in the summer (black) and winter (light blue). Percent contributions of on-road heavy-duty diesel vehicles (HDDVs) to NO_x emission density-based LIN-HIW inequalities during summer months from the FIVE18–19 and NEI17 (b). The mean HDDV contribution to emissions inequality, weighted by UA population, is also displayed.

(*r*) of 0.82 for the combined race-ethnicity and income metric (LIN-HIW). At the same time, relative inequalities (%) are only moderately associated with city-level NO₂ (*r* = 0.46), suggesting that sustained NO_x emission control will reduce but not eliminate NO₂ disparities, a result consistent with work investigating trends in NO₂ inequality between 2000 and 2010 using land-use regression NO₂ data sets (Clark et al., 2017) and before and during COVID-19-related activity changes using TROPOMI NO₂ TVCDs (Kerr et al., 2021).

To observationally constrain city-wide effective contributions of HDDVs to NO₂ disparities, we first compare TROPOMI NO₂ inequalities on weekdays and weekends and then contextualize the measured changes using NO_x emission weekday-weekend patterns predicted by the FIVE18–19 (mobile sources) and NEI17 (point sources). HDDVs transport commercial goods and their emissions are substantially reduced on weekends; at the same time, passenger vehicles (largely gasoline-powered in the United States) and point source emissions exhibit much less weekday-weekend variability, although the timing of their emissions may change (Marr & Harley, 2002; McDonald et al., 2014; Russell et al., 2012). Off-road diesel engines (e.g., construction) also vary weekday to weekend; however, their contribution to total urban NO_x emissions is considerably smaller than on-road HDDVs. While HDDVs with NO_x control are a growing portion of the vehicle fleet (Jiang et al., 2018), with reports of declining weekday-weekend NO₂ differences (Demetillo et al., 2019), HDDVs still emit an important fraction of urban NO_x. In the 52 UAs at the focus of this work, NO₂ TVCDs are an average of 34 ± 17% (1σ standard deviation) lower on weekends than weekdays (June 2018–February 2020).

Weekday-weekend differences in city-level census-tract absolute TROPOMI NO₂ inequalities are fit using a weighted bivariate linear regression model (York et al., 2004), with weights derived from errors in city-level NO₂ for the different residential populations (Table S4). Because NO₂ concentrations better correlate with NO_x emission rates when the NO₂ atmospheric lifetime is short, we evaluate correlations separately in the summer and winter. We determine the ‘effective’ HDDV contribution to inequalities from the regression slope, which is a combined function of changes in both the total NO_x emissions and the nonlinear NO₂-dependent NO₂ chemical lifetime. This method weights cities equally regardless of population. LIN-HIW disparities decrease by 37 ± 3% on weekends in the summer and 32 ± 2% in the winter (Figure 2a). Weekday and weekend inequalities are more strongly correlated in the summer (*r* = 0.93) than winter (*r* = 0.51), a function of seasonal differences in NO₂ lifetime and reduced wintertime sampling statistics. For race-ethnicity and poverty metrics, weekday-weekend differences are 28%–46% in the summer (mapped in Figure S2) and more variable in the winter (0%–41%). We observe weekend NO₂ decreases to be spatially variable within cities and larger in census tracts where residents are primarily people of color or have lower

household incomes. Weekday-weekend NO_2 differences indicate greater weekend NO_x emission reductions in the most polluted neighborhoods, as summertime weekend NO_2 decreases are 50% larger in the highest quintile NO_2 census tracts than the lowest quintile NO_2 tracts. Comparable weekday-weekend decreases are observed in the winter for the highest and lowest quintile NO_2 tracts, consistent with longer NO_2 lifetimes and NO_2 TVCDs being more distributed from NO_x emission sources in space and time.

Observed weekday-weekend differences in NO_2 TVCDs are a function of both the direct change in NO_x emissions and the subsequent indirect effects on the NO_x -dependent NO_2 lifetime. Weekday-weekend differences in NO_x emissions are driven by the fraction of total HDDVs that are parked on weekends, and, to a smaller extent, concurrent changes in spatiotemporal patterns of other vehicle types. To attribute measured differences in NO_2 disparities to a specific reduction in diesel traffic, we compare TROPOMI-based results with changes in NO_x emission densities (metric tons $\text{NO}_x \text{ day}^{-1} \text{ km}^{-2}$), and their resulting inequalities, derived from the FIVE18–19 and NEI17. We first degrade the $0.01^\circ \times 0.01^\circ$ oversampled TROPOMI product and FIVE18–19 database ($4 \times 4 \text{ km}^2$) to the same $0.04^\circ \times 0.04^\circ$ grid, average each to underlying census tracts, and calculate inequalities as described in Section 2.2. NEI17 sources are represented as points and summed within their respective tracts. Tract-level FIVE18–19 and NEI17 are combined and normalized by tract areas to produce NO_x emissions densities. We analyze inventory-based results, and their comparison with TROPOMI, separately in the summer and winter.

Because we expect the coarser $0.04^\circ \times 0.04^\circ$ grid to influence the observed inter-tract differences, we first compare tract-averaged disparities based on the $0.01^\circ \times 0.01^\circ$ oversampled TVCDs to those determined using the $0.04^\circ \times 0.04^\circ$ TVCDs. We calculate the normalized mean biases and errors in the absolute and relative inequalities separately on summer and winter weekdays, using the $0.01^\circ \times 0.01^\circ$ TROPOMI-based results as our reference values. Despite the loss of spatial detail, US-wide normalized mean biases for the different inequality metrics are just <1%–6% (Figure S1 and Table S5). We generally calculate slightly higher NO_2 inequalities with the coarser-resolution NO_2 product than the $0.01^\circ \times 0.01^\circ$ TVCDs, suggesting larger pixels have the effect of distributing NO_x emissions over spatial areas with similar demographic and income characteristics. The greatest city-level normalized mean biases (8%–22%) are observed in Oakland, San Diego, and San Francisco, CA, all cities that encompass narrow geographical areas along coasts that may even challenge the satellite analysis at $0.01^\circ \times 0.01^\circ$. While normalized mean biases are low on average across UAs, normalized mean errors for each metric are higher (3%–13%), indicating inaccuracies are larger in individual cities because of the loss of spatial resolution. That said, we find the $0.04^\circ \times 0.04^\circ$ TVCDs give comparable weekday-weekend NO_2 differences to the $0.01^\circ \times 0.01^\circ$ product for all inequality metrics (Table S4). Coarse-resolution TVCDs yield weekday-weekend decreases in LIN-HIW disparities of $37 \pm 4\%$ and $38 \pm 2\%$ in the summer and winter, respectively, equaling results with the $0.01^\circ \times 0.01^\circ$ TVCDs within uncertainties in the summer. Agreement is similar for the other metrics, indicating data sets resolved to $0.04^\circ \times 0.04^\circ$ still capture tract-scale patterns in the intra-urban spatiotemporal distribution.

Using the FIVE18–19 and NEI17, we calculate mean summertime weekday-weekend reductions in LIN-HIW disparities in NO_x emissions densities of $40 \pm 4\%$ (includes all source sectors), in agreement with TROPOMI-based weekday-weekend differences using the $0.04^\circ \times 0.04^\circ$ TVCDs within associated uncertainties (Table S4). For race-ethnicity and poverty status, weekday to weekend decreases in emissions disparities equal empirical estimates to within 3%–15%, with the inventories generally predicting comparable or slightly larger weekend reductions than TROPOMI. There is larger disagreement between NO_2 TVCDs and the inventories in the winter, with TROPOMI weekday-weekend differences for some race-ethnicity metrics being much smaller than estimated by the FIVE18–19 and NEI17. These wintertime discrepancies are consistent with seasonal patterns in NO_2 mesoscale transport (greater day-to-day carryover), farther NO_2 displacement away from NO_x sources, and more NO_x -suppressed chemistry, but may also be related to the reduced wintertime sampling statistics on weekdays and weekends.

Finally, we partition NO_x emission inequalities and their weekday-weekend differences by source sector, focusing on the role of HDDVs. We limit the analysis to summer months, when NO_2 TVCDs are most responsive to NO_x emissions changes. On weekdays, on-road HDDVs cause on average (unweighted by UA population) $45 \pm 5\%$ of LIN-HIW NO_x emissions-based inequalities (Figure 2b and Table S7). The remainder is due to on-road gasoline-powered vehicles ($38 \pm 5\%$), gasoline and diesel off-road vehicles ($13 \pm 6\%$), and stationary sources ($4 \pm 6\%$), largely electricity generation. HDDVs contribute significantly to mean (weighted by

UA population) NO_x emissions inequalities for Black and African Americans ($63 \pm 13\%$), Hispanics/Latinos ($52 \pm 10\%$), Asians ($36 \pm 7\%$), and Native Americans ($62 \pm 12\%$) and for people living below and near the poverty line ($56 \pm 11\%$) (Figure S3). While HDDVs are the largest source of UA-level disparities, stationary sources may be more important across more suburban metropolitan areas. Regulatory controls on gasoline-powered vehicles and electricity generation between 2000 and 2010 decreased absolute, although not relative, NO₂ inequalities from these sources across the United States (Clark et al., 2017), and an analysis exploiting COVID-19-related reductions in passenger vehicle traffic suggest HDDV emissions dominate relative NO₂ inequalities in recent years (Kerr et al., 2021). Based on the FIVE18–19, summertime HDDV NO_x emission densities decrease by $62 \pm 2\%$ on weekends, with diesel traffic still causing $26 \pm 6\%$ of LIN-HIW NO_x emissions inequalities on weekends. Therefore, if the entire observed effective weekday-weekend change in NO₂ TVCD disparities is caused by HDDVs, then a $62 \pm 2\%$ reduction in summertime weekday on-road HDDV emissions leads to a $37 \pm 3\%$ decrease in NO₂ LIN-HIW disparities. While we find that on average LIN-HIW NO_x emission densities from the other major source of emissions-based inequalities, gasoline-powered vehicles, decrease by 10% weekday to weekend, NO_x emission inequalities change by less than 1% (Table S6), indicating that weekday-weekend differences in disparities are driven by HDDVs. If HDDV emissions were fully controlled—or their distribution was equalized—summer weekday LIN-HIW NO_x emissions inequalities would decrease by almost 50%. Likewise, elimination of on-road HDDV inequalities would lower disparities with race-ethnicity and poverty by 59% and 49%, respectively (Table S7). These predicted changes represent upper bounds, as US urban chemical oxidation is trending toward NO_x-limitation (Laughner & Cohen, 2019).

3.2. Resolving Census Tract-Scale Inequality From Space

Application of satellite remote sensing to NO₂ inequality requires demonstration that both oversampled TROPOMI TVCDs capture inter-census-tract differences and that spatial patterns in NO₂ columns reflect those that would be measured at the surface. In Demetillo et al. (2020), we found TROPOMI-based results were comparable to NO₂ tract-scale disparities determined using the high spatial resolution airborne sensor GCAS in Houston, TX, and used in situ NO₂ aircraft profiles and surface data to show the spatial patterns in NO₂ columns reflected those at the surface. Because we do not have aircraft measurements for the 52 cities in our domain, we instead test the dependence of tract-level NO₂ inequalities on spatial heterogeneities in UA demographics. To evaluate relationships between column and surface NO₂ spatial distributions, we analyze Pearson correlation coefficients of TVCDs and surface NO₂* mixing ratios as a function of observation proximity.

Because of historical and contemporary racial discrimination, US cities are segregated by race, ethnicity, and income—without segregation, air pollution disparities would not be possible. We find city-level race-ethnicity NO₂ inequalities are weakly associated with overall segregation extent ($r = 0.35$; $p = 0.010$) (Figure S4), suggesting UAs are sufficiently segregated to support intra-urban NO₂ disparities, and those NO₂ inequalities are more sensitive to changes in overall NO₂ pollution level. Segregation structure can be characterized along an axis between clustered segregation, where segregated tracts spatially aggregate into larger contiguous regions, and patch-worked segregation, where the spatial scale of segregated tracts is small and adjacent tracts are more likely to have different demographic populations (Chodrow, 2017; Lee et al., 2008; Reardon & O'Sullivan, 2004). For reference, Atlanta, GA typifies clustering, while New York City, NY exhibits patch-worked segregation (Figure S5). This structural distinction is informative for the application of TROPOMI, as the $0.01^\circ \times 0.01^\circ$ spatial resolution is coarser than many densely populated tracts and oversampling has the effect of smoothing spatial gradients through averaging. Because NO₂ spatially varies at sub-census-tract scales (e.g., Messier et al., 2018; Miller et al., 2020), if the tract unit challenges the TROPOMI resolution, NO₂ disparities would positively correlate with increased clustering, providing a test of the TROPOMI resolution at the tract scale. Here, we compare race-ethnicity summer weekday NO₂ inequalities with urban race-ethnicity segregation structure (Figure S4). We find that city-level race-ethnicity NO₂ disparities are uncorrelated with segregation structure ($r = 0.07$, $p = 0.619$) and not positively associated with clustering, implying TROPOMI is indeed able to resolve inter-tract differences even when segregated tracts do not spatially aggregate. Past research has shown city-level NO₂ co-varies with urban form and density (Bechle et al., 2011, 2017; Larkin et al., 2017). However, because we focus on the urban core, we cross-cut this variability, largely excluding urban-suburban form and density gradients.

To assess whether spatial distributions in NO₂ TVCDs reflect those at the surface, we compare NO₂ columns and mean daytime (12–3 p.m. LT) NO₂* surface mixing ratios as a function of the spatial proximity between tract-averaged TVCDs and the NO₂* nearest monitor (Figure S6) (Bechle et al., 2013; Demetillo et al., 2020). Census tract coverage is spatially continuous; however, there are instances where no tracts are identified within a given 1-km interval (*i*). Here, tract-averaged TVCDs are set equal to the column value in the *i* + 1 distance interval, or infrequently the *i* + 2 interval. This largely occurs when comparing directly overhead tract-averaged TVCDs, so we limit the correction to columns ≤1 km from the nearest NO₂* monitor. The highest mean *r* values are observed when TVCDs and surface measurements are spatially coincident, 0.69 ± 0.05 in the summer and 0.60 ± 0.09 in the winter. However, we anticipate that *r* values (≤1 km) would be even higher if comparisons were instead based on the 0.01° × 0.01° product. At distances of 6–10 km, *r* values fall to 0.42 ± 0.07 (summer) and 0.30 ± 0.09 (winter). These results indicate that TROPOMI TVCDs capture similar spatial patterns as measured at the surface, but also highlight that the NO₂* network is too spatially sparse to collect locally relevant NO₂* levels for most residents.

4. Summary

We use TROPOMI observations to quantify NO₂ inequality in 52 major US cities over June 2018–February 2020. We report average census tract-level population-weighted NO₂ disparities for Black and African Americans (17 ± 2%), Hispanics/Latinos (19 ± 2%), Asians (12 ± 2%), and Native Americans (15 ± 2%) compared to non-Hispanic/Latino whites, and for people living below (17 ± 2%) and near the poverty line (10 ± 2%) compared to those living above. Higher inequalities are found when race-ethnicity and income are combined, with 28 ± 2% greater population-weighted NO₂ for LINs than HIWs. For all metrics, much greater disparities are observed in some larger US cities. Absolute NO₂ inequalities are strongly associated with UA NO₂ pollution; however, correlations between relative inequalities and city-level NO₂ are weaker. We use weekday-weekend differences in NO₂ TVCDs as empirical constraints on the impact of regulating HDDV NO_x emissions, showing that a 62% reduction in on-road diesel traffic leads to a 37% decrease in LIN-HIW inequalities. While HDDV emissions contribute to the majority of NO₂ inequalities—63 ± 13% for Black and African Americans, 52 ± 10% for Hispanics/Latinos, 36 ± 7% for Asians, 62 ± 12% for Native Americans, and 56 ± 11% for people living below or near the poverty line—controlling them entirely would not eliminate NO₂ disparities. Finally, we provide additional evidence that oversampled TROPOMI observations resolve key patterns in the census tract-scale NO₂ distribution with NO₂ disparities being invariant with segregation structure and that spatial patterns in directly overhead NO₂ columns reflect surface-level NO₂ spatial patterns.

Data Availability Statement

TROPOMI NO₂ Level 2 TVCDs can be accessed at <https://earthdata.nasa.gov/earth-observation-data>. EPA NO₂* surface data can be downloaded at https://aqs.epa.gov/aqsweb/airdata/download_files.html. The US Census database is accessible from the IPUMS National Historical Geographic Information System (<https://www.nhgis.org>) and census tract polygons are available as TIGER/Line shapefiles from the Data.gov library (<https://www.census.gov/cgi-bin/geo/shapefiles/index.php>). The NEI17 can be accessed at <https://www.epa.gov/air-emissions-inventories/2017-national-emissions-inventory-nei-data> and the FIVE18–19 is available for download at the NOAA Chemical Sciences Laboratory COVID-AQS database (<https://csl.noaa.gov/groups/csl7/measurements/2020covid-aqs/emissions/>).

References

- Adar, S. D., & Kaufman, J. D. (2007). Cardiovascular disease and air pollutants: Evaluating and improving epidemiological data implicating traffic exposure. *Inhalation Toxicology*, 19, 135–149. <https://doi.org/10.1080/08958370701496012>
- Apte, J. S., Messier, K. P., Gani, S., Brauer, M., Kirchstetter, T. W., Lunden, M. M., et al. (2017). High-resolution air pollution mapping with Google Street View cars: Exploiting big data. *Environmental Science & Technology*, 51(12), 6999–7008. <https://doi.org/10.1021/acs.est.7b00891>
- Ard, K. (2015). Trends in exposure to industrial air toxins for different racial and socioeconomic groups: A spatial and temporal examination of environmental inequality in the U.S. from 1995 to 2004. *Social Science Research*, 53, 375–390. <https://doi.org/10.1016/j.ssresearch.2015.06.019>

Acknowledgments

This study was funded by the NASA New Investigator Program in Earth Science (20-NIP20-0056) and an NSF CAREER Award (AGS 2047150) to SEP. MAGD was supported by a NASA Future Investigator NASA Earth and Space Science and Technology (FINESST) Graduate Research Fellowship (19-EARTH20-0242) and the Virginia Space Grant Consortium. The FIVE18–19 mobile source inventory was developed with support from NOAA NRDD Project 19533.

- Bechle, M. J., Millet, D. B., & Marshall, J. D. (2011). Effects of income and urban form on urban NO₂: Global evidence from satellites. *Environmental Science & Technology*, 45(11), 4914–4919. <https://doi.org/10.1021/es103866b>
- Bechle, M. J., Millet, D. B., & Marshall, J. D. (2013). Remote sensing of exposure to NO₂: Satellite versus ground-based measurement in a large urban area. *Atmospheric Environment*, 69, 345–353. <https://doi.org/10.1016/j.atmosenv.2012.11.046>
- Bechle, M. J., Millet, D. B., & Marshall, J. D. (2017). Does urban form affect urban NO₂? Satellite-based evidence for more than 1200 cities. *Environmental Science & Technology*, 51(21), 12707–12716. <https://doi.org/10.1021/acs.est.7b01194>
- Bell, M. L., & Ebisu, K. (2012). Environmental inequality in exposures to airborne particulate matter components in the United States. *Environmental Health Perspectives*, 120(12), 1699–1704. <https://doi.org/10.1289/ehp.1205201>
- Boersma, K. F., Eskes, H. J., Dirksen, R. J., van der A, R. J., Veefkind, J. P., Stammes, P., et al. (2011). An improved tropospheric NO₂ column retrieval algorithm for the ozone monitoring instrument. *Atmospheric Measurement Techniques*, 4(9), 1905–1928. <https://doi.org/10.5194/amt-4-1905-2011>
- Boersma, K. F., Eskes, H. J., Richter, A., De Smedt, I., Lorente, A., Beirle, S., et al. (2018). Improving algorithms and uncertainty estimates for satellite NO₂ retrievals: Results from the quality assurance for the essential climate variables (QA4ECV) project. *Atmospheric Measurement Techniques*, 11(12), 6651–6678. <https://doi.org/10.5194/amt-11-6651-2018>
- Brook, J. R., Burnett, R. T., Dann, T. F., Cakmak, S., Goldberg, M. S., Fan, X. H., & Wheeler, A. J. (2007). Further interpretation of the acute effect of nitrogen dioxide observed in Canadian time-series studies. *Journal of Exposure Science and Environmental Epidemiology*, 17, S36–S44. <https://doi.org/10.1038/sj.jes.7500626>
- Brunekreef, B., & Holgate, S. T. (2002). Air pollution and health. *Lancet*, 360(9341), 1233–1242. [https://doi.org/10.1016/S0140-6736\(02\)11274-8](https://doi.org/10.1016/S0140-6736(02)11274-8)
- Bullard, R. D. (1987). *Invisible Houston: The black experience in boom and bust*. College Station: Texas A & M University Press.
- Burnett, R. T., Stieb, D., Brook, J. R., Cakmak, S., Dales, R., Raizenne, M., et al. (2004). Associations between short-term changes in nitrogen dioxide and mortality in Canadian cities. *Archives of Environmental & Occupational Health*, 59(5), 228–236. <https://doi.org/10.3200/aeoh.59.5.228-236>
- Chodrow, P. S. (2017). Structure and information in spatial segregation. *Proceedings of the National Academy of Sciences of the United States of America*, 114(44), 11591–11596. <https://doi.org/10.1073/pnas.1708201114>
- Choi, W., He, M., Barbesant, V., Kozawa, K., Mara, S., Winer, A., & Paulson, S. (2012). Prevalence of wide area impacts downwind of freeways under pre-sunrise stable atmospheric conditions. *Atmospheric Environment*, 62, 318–327. <https://doi.org/10.1016/j.atmosenv.2012.07.084>
- Clark, L. P., Millet, D. B., & Marshall, J. D. (2014). National patterns in environmental injustice and inequality: Outdoor NO₂ air pollution in the United States. *PLOS One*, 9(4), e94431. <https://doi.org/10.1371/journal.pone.0094431>
- Clark, L. P., Millet, D. B., & Marshall, J. D. (2017). Changes in transportation-related air pollution exposures by race-ethnicity and socioeconomic status: Outdoor nitrogen dioxide in the United States in 2000 and 2010. *Environmental Health Perspectives*, 125(9), 097012. <https://doi.org/10.1289/ehp959>
- Demetillo, M. A. G., Anderson, J. F., Geddes, J. A., Najacht, E., Herrera, S. A., Kabasares, K., et al. (2019). Observing severe drought influences on ozone air pollution in California. *Environmental Science & Technology*, 53(9), 4695–4706. <https://doi.org/10.1021/acs.est.8b04852>
- Demetillo, M. A. G., Navarro, A., Knowles, K. K., Fields, K. P., Geddes, J. A., Nowlan, C. R., et al. (2020). Observing nitrogen dioxide air pollution inequality using high-spatial-resolution remote sensing measurements in Houston, Texas. *Environmental Science & Technology*, 54(16), 9882–9895. <https://doi.org/10.1021/acs.est.0c01864>
- Di, Q., Wang, Y., Zanobetti, A., Wang, Y., Koutrakis, P., Choirat, C., et al. (2017). Air pollution and mortality in the medicare population. *The New England Journal of Medicine*, 376(26), 2513–2522. <https://doi.org/10.1056/nejmoa1702747>
- Dunlea, E. J., Herndon, S. C., Nelson, D. D., Volkamer, R. M., San Martini, F., Sheehy, P. M., et al. (2007). Evaluation of nitrogen dioxide chemiluminescence monitors in a polluted urban environment. *Atmospheric Chemistry and Physics*, 7(10), 2691–2704. <https://doi.org/10.5194/acp-7-2691-2007>
- Environmental Protection Agency (EPA). (2021). Retrieved from <https://www.epa.gov/air-emissions-inventories/2017-national-emissions-inventory-nei-data>
- Federal Highway Administration (FHWA). (2020). *HPMS public release*. (p. 2018). Office of Highway Policy Information, Federal Highway Administration, U.S. Department of Transportation.
- Frost, G. J., McKeen, S. A., Trainer, M., Ryerson, T. B., Neuman, J. A., Roberts, J. M., et al. (2006). Effects of changing power plant NO_x emissions on ozone in the eastern United States: Proof of concept. *Journal of Geophysical Research - D: Atmospheres*, 111(D12), D12306. <https://doi.org/10.1029/2005jd006354>
- Gwynn, R. C., & Thurston, G. D. (2001). The burden of air pollution: Impacts among racial minorities. *Environmental Health Perspectives*, 109, 501–506. <https://doi.org/10.2307/3454660>
- Harkins, C., McDonald, B. C., Henze, D. K., & Wiedinmyer, C. (2021). A fuel-based method for updating mobile source emissions during the COVID-19 pandemic. *Environmental Research Letters*, 16, 065018. <https://doi.org/10.1088/1748-9326/ac0660>
- Health Effects Institute (HEI). (2010). *Traffic-related air pollution: A critical review of the literature on emissions, exposure, and health effects* (Special report 17).
- Houston, D., Krudysz, M., & Winer, A. (2008). Diesel truck traffic in low-income and minority communities adjacent to ports: Environmental justice implications of near-roadway land use conflicts. *Transportation Research Record*, 2067(1), 38–46. <https://doi.org/10.3141/2067-05>
- Houston, D., Li, W., & Wu, J. (2014). Disparities in exposure to automobile and truck traffic and vehicle emissions near the Los Angeles–Long Beach port complex. *American Journal of Public Health*, 104(1), 156–164. <https://doi.org/10.2105/ajph.2012.301120>
- Houston, D., Ong, P., Jaimes, G., & Winer, A. (2011). Traffic exposure near the Los Angeles–Long Beach port complex: Using GPS-enhanced tracking to assess the implications of unreported travel and locations. *Journal of Transport Geography*, 19(6), 1399–1409. <https://doi.org/10.1016/j.jtrangeo.2011.07.018>
- Houston, D., Wu, J., Ong, P., & Winer, A. (2004). Structural disparities of urban traffic in Southern California: Implications for vehicle-related air pollution exposure in minority and high-poverty neighborhoods. *Journal of Urban Affairs*, 26(5), 565–592. <https://doi.org/10.1111/j.0735-2166.2004.00215.x>
- Jerrett, M., Burnett, R. T., Ma, R. J., Pope, C. A., Krewski, D., Newbold, K. B., et al. (2005). Spatial analysis of air pollution and mortality in Los Angeles. *Epidemiology*, 16(6), 727–736. <https://doi.org/10.1097/01.ede.0000181630.15826.7d>

- Jiang, Z., McDonald, B. C., Worden, H., Worden, J. R., Miyazaki, K., Qu, Z., et al. (2018). Unexpected slowdown of US pollutant emission reduction in the past decade. *Proceedings of the National Academy of Sciences of the United States of America*, *115*(20), 5099–5104. <https://doi.org/10.1073/pnas.1801191115>
- Karner, A. A., Eisinger, D. S., & Niemeier, D. A. (2010). Near-roadway air quality: Synthesizing the findings from real-world data. *Environmental Science & Technology*, *44*(14), 5334–5344. <https://doi.org/10.1021/es100008x>
- Kerr, G. H., Goldberg, D. H., & Anenberg, S. C. (2021). COVID-19 pandemic reveals persistent disparities in nitrogen dioxide pollution. *Proceedings of the National Academy of Sciences of the United States of America*, *118*(30), e2022409118. <https://doi.org/10.1073/pnas.2022409118>
- Kleipool, Q. L., Dobber, M. R., de Haan, J. F., & Levelt, P. F. (2008). Earth surface reflectance climatology from 3 years of OMI data. *Journal of Geophysical Research - D: Atmospheres*, *113*(D18), D18308. <https://doi.org/10.1029/2008jd010290>
- Kravitz-Wirtz, N., Crowder, K., Hajat, A., & Sass, V. (2016). The long-term dynamics of racial/ethnic inequality in neighborhood air pollution exposure, 1990–2009. *Du Bois Review*, *13*(2), 237–259. <https://doi.org/10.1017/s1742058x16000205>
- Larkin, A., Geddes, J. A., Martin, R. V., Xiao, Q., Liu, Y., Marshall, J. D., et al. (2017). Global land use regression model for nitrogen dioxide air pollution. *Environmental Science & Technology*, *51*(12), 6957–6964. <https://doi.org/10.1021/acs.est.7b01148>
- Laughner, J. L., & Cohen, R. C. (2019). Direct observation of changing NO_x lifetime in North American cities. *Science*, *366*(6466), 723–727. <https://doi.org/10.1126/science.aax6832>
- Lee, B. A., Reardon, S. F., Firebaugh, G., Farrell, C. R., Matthews, S. A., & O'Sullivan, D. (2008). Beyond the census tract: Patterns and determinants of racial segregation at multiple geographic scales. *American Sociological Review*, *73*(5), 766–791. <https://doi.org/10.1177/000312240807300504>
- Lena, T. S., Ochieng, V., Carter, M., Holguin-Veras, J., & Kinney, P. L. (2002). Elemental carbon and PM_{2.5} levels in an urban community heavily impacted by truck traffic. *Environmental Health Perspectives*, *110*(10), 1009–1015. <https://doi.org/10.1289/ehp.021101009>
- Levy, I., Mihele, C., Lu, G., Narayan, J., & Brook, J. R. (2014). Evaluating multipollutant exposure and urban air quality: Pollutant interrelationships, neighborhood variability, and nitrogen dioxide as a proxy pollutant. *Environmental Health Perspectives*, *122*(1), 65–72. <https://doi.org/10.1289/ehp.1306518>
- Levy, J. I., Greco, S. L., Melly, S. J., & Mukhi, N. (2009). Evaluating efficiency-equality tradeoffs for mobile source control Strategies in an urban area. *Risk Analysis*, *29*(1), 34–47. <https://doi.org/10.1111/j.1539-6924.2008.01119.x>
- Lin, S., Munsie, J. P., Hwang, S. A., Fitzgerald, E., & Cayo, M. R. (2002). Childhood asthma hospitalization and residential exposure to state route traffic. *Environmental Research*, *88*(2), 73–81. <https://doi.org/10.1006/enrs.2001.4303>
- Lipfert, F. W., & Wyzga, R. E. (2008). On exposure and response relationships for health effects associated with exposure to vehicular traffic. *Journal of Exposure Science and Environmental Epidemiology*, *18*(6), 588–599. <https://doi.org/10.1038/jes.2008.4>
- Lorente, A., Folkert Boersma, K., Yu, H., Dörner, S., Hilboll, A., Richter, A., et al. (2017). Structural uncertainty in air mass factor calculation for NO₂ and HCHO satellite retrievals. *Atmospheric Measurement Techniques*, *10*(3), 759–782. <https://doi.org/10.5194/amt-10-759-2017>
- Marr, L. C., & Harley, R. A. (2002). Modeling the effect of weekday–weekend differences in motor vehicle emissions on photochemical air pollution in Central California. *Environmental Science & Technology*, *36*(19), 4099–4106. <https://doi.org/10.1021/es020629x>
- McDonald, B. C., Dallmann, T. R., Martin, E. W., & Harley, R. A. (2012). Long-term trends in nitrogen oxide emissions from motor vehicles at national, state, and air basin scales. *Journal of Geophysical Research - D: Atmospheres*, *117*(D21), D00V18. <https://doi.org/10.1029/2012jd018304>
- McDonald, B. C., McBride, Z. C., Martin, E. W., & Harley, R. A. (2014). High-resolution mapping of motor vehicle carbon dioxide emissions. *Journal of Geophysical Research - D: Atmospheres*, *119*(9), 5283–5298. <https://doi.org/10.1002/2013jd021219>
- McDonald, B. C., McKeen, S. A., Cui, Y. Y., Ahmadov, R., Kim, S.-W., Frost, G. J., et al. (2018). Modeling ozone in the Eastern U.S. using a fuel-based mobile source emissions inventory. *Environmental Science & Technology*, *52*(13), 7360–7370. <https://doi.org/10.1021/acs.est.8b00778>
- Messier, K. P., Chambliss, S. E., Gani, S., Alvarez, R., Brauer, M., Choi, J. J., et al. (2018). Mapping air pollution with Google Street View cars: Efficient approaches with mobile monitoring and land use regression. *Environmental Science & Technology*, *52*(21), 12563–12572. <https://doi.org/10.1021/acs.est.8b03395>
- Miller, D. J., Actkinson, B., Padilla, L., Griffin, R. J., Moore, K., Lewis, P. G. T., et al. (2020). Characterizing elevated urban air pollutant spatial patterns with mobile monitoring in Houston, Texas. *Environmental Science & Technology*, *54*(4), 2133–2142. <https://doi.org/10.1021/acs.est.9b05523>
- Nguyen, N. P., & Marshall, J. D. (2018). Impact, efficiency, inequality, and injustice of urban air pollution: Variability by emission location. *Environmental Research Letters*, *13*(2), 024002.
- Nowlan, C. R., Liu, X., Janz, S. J., Kowalewski, M. G., Chance, K., Follette-Cook, M. B., et al. (2018). Nitrogen dioxide and formaldehyde measurements from the GEOstationary Coastal and Air Pollution Events (GEO-CAPE) airborne simulator over Houston, Texas. *Atmospheric Measurement Techniques*, *11*(11), 5941–5964. <https://doi.org/10.5194/amt-11-5941-2018>
- O'Neill, M. S., Jerrett, M., Kawachi, L., Levy, J. L., Cohen, A. J., Gouveia, N., et al. (2003). Health, wealth, and air pollution: Advancing theory and methods. *Environmental Health Perspectives*, *111*(16), 1861–1870. <https://doi.org/10.1289/ehp.6334>
- Pope, R., Wu, J., & Boone, C. (2016). Spatial patterns of air pollutants and social groups: A distributive environmental justice study in the phoenix metropolitan region of USA. *Environmental Management*, *58*(5), 753–766. <https://doi.org/10.1007/s00267-016-0741-z>
- Reardon, S. F., & Firebaugh, G. (2002). Measures of multigroup segregation. *Sociological Methodology*, *32*(1), 33–67. <https://doi.org/10.1111/1467-9531.00110>
- Reardon, S. F., & O'Sullivan, D. (2004). Measures of spatial segregation. *Sociological Methodology*, *34*(1), 121–162. <https://doi.org/10.1111/j.0081-1750.2004.00150.x>
- Roberto, E. (2015). *Measuring inequality and segregation*. arXiv:1508.01167 (pp. 1–26).
- Rosofsky, A., Levy, J. I., Zanobetti, A., Janulewicz, P., & Fabiana, M. P. (2018). Temporal trends in air pollution exposure inequality in Massachusetts. *Environmental Research*, *161*, 76–86. <https://doi.org/10.1016/j.envres.2017.10.028>
- Russell, A. R., Valin, L. C., Bucsel, E. J., Wenig, M. O., & Cohen, R. C. (2010). Space-based constraints on spatial and temporal patterns of NO_x emissions in California, 2005–2008. *Environmental Science & Technology*, *44*(9), 3608–3615. <https://doi.org/10.1021/es903451j>
- Russell, A. R., Valin, L. C., & Cohen, R. C. (2012). Trends in OMI NO₂ observations over the United States: Effects of emission control technology and the economic recession. *Atmospheric Chemistry and Physics*, *12*, 12197–12209. <https://doi.org/10.5194/acp-12-12197-2012>
- Southerland, V. A., Anenberg, S. C., Harris, M., Apte, J., Hystad, P., van Donkelaar, A., et al. (2021). Assessing the distribution of air pollution health risks within cities: A neighborhood-scale analysis leveraging high-resolution data sets in the Bay Area, California. *Environmental Health Perspectives*, *129*(3). <https://doi.org/10.1289/EHP7679>

- Sun, K., Zhu, L., Cady-Pereira, K., Chan Miller, C., Chance, K., Clarisse, L., et al. (2018). A physics-based approach to oversample multi-satellite, multispecies observations to a common grid. *Atmospheric Measurement Techniques*, *11*(12), 6679–6701. <https://doi.org/10.5194/amt-11-6679-2018>
- Tessum, C. W., Apte, J. S., Goodkind, A. L., Muller, N. Z., Mullins, K. E., Paoletta, D. A., et al. (2019). Inequity in consumption of goods and services adds to racial–ethnic disparities in air pollution exposure. *Proceedings of the National Academy of Sciences of the United States of America*, *116*(13), 6001–6006. <https://doi.org/10.1073/pnas.1818859116>
- Tessum, C. W., Paoletta, D. A., Chambliss, S. E., Apte, J. S., Hill, J. D., & Marshall, J. D. (2021). PM_{2.5} pollutants disproportionately and systemically affect people of color in the United States. *Science Advances*, *7*, eabf4491. <https://doi.org/10.1126/sciadv.abf4491>
- Theil, H., & Finizza, A. J. (1971). A note on the measurement of racial integration of schools by means of informational concepts. *Journal of Mathematical Sociology*, *1*(2), 187–193. <https://doi.org/10.1080/0022250x.1971.9989795>
- van Geffen, J. H. G. M., Boersma, K. F., Eskes, H. J., Maasakkers, J. D., & Veeffkind, J. P. (2018). TROPOMI ATBD of the total and tropospheric NO₂ data products. Retrieved from <http://www.tropomi.eu>
- van Geffen, J. H. G. M., Boersma, K. F., Van Roozendaal, M., Hendrick, F., Mahieu, E., De Smedt, I., et al. (2015). Improved spectral fitting of nitrogen dioxide from OMI in the 405–465 nm window. *Atmospheric Measurement Techniques*, *8*(4), 1685–1699. <https://doi.org/10.5194/amt-8-1685-2015>
- Veeffkind, J. P., Aben, I., McMullan, K., Förster, H., de Vries, J., Otter, G., et al. (2012). TROPOMI on the ESA Sentinel-5 Precursor: A GMES mission for global observations of the atmospheric composition for climate, air quality and ozone layer applications. *Remote Sensing of Environment*, *120*, 70–83. <https://doi.org/10.1016/j.rse.2011.09.027>
- Williams, J. E., Boersma, K. F., Le Sager, P., & Verstraeten, W. W. (2017). The high-resolution version of TM5-MP for optimized satellite retrievals: Description and validation. *Geoscientific Model Development*, *10*(2), 721–750. <https://doi.org/10.5194/gmd-10-721-2017>
- York, D., Evensen, N. M., Martínez, M. L., & Delgado, J. D. B. (2004). Unified equations for the slope, intercept, and standard errors of the best straight line. *American Journal of Physics*, *72*(3), 367–375. <https://doi.org/10.1119/1.1632486>
- Zara, M., Boersma, K. F., De Smedt, I., Richter, A., Peters, E., van Geffen, J. H. G. M., et al. (2018). Improved slant column density retrieval of nitrogen dioxide and formaldehyde for OMI and GOME-2A from QA4ECV: Intercomparison, uncertainty characterisation, and trends. *Atmospheric Measurement Techniques*, *11*(7), 4033–4058. <https://doi.org/10.5194/amt-11-4033-2018>